



OPEN

AI-enabled ECG index for predicting left ventricular dysfunction in patients with ST-segment elevation myocardial infarction

Ki-Hyun Jeon^{1,4}✉, Hak Seung Lee^{2,3,4}✉, Sora Kang^{2,3}, Jong-Hwan Jang^{2,3}, Yong-Yeon Jo^{2,3}, Jeong Min Son^{2,3}, Min Sung Lee^{2,3}, Joon-myoung Kwon^{2,3}, Ju-Seung Kwun¹, Hyoung-Won Cho¹, Si-Hyuck Kang¹, Wonjae Lee¹, Chang-Hwan Yoon¹, Jung-Won Suh¹, Tae-Jin Youn¹ & In-Ho Chae¹

Electrocardiogram (ECG) changes after primary percutaneous coronary intervention (PCI) in ST-segment elevation myocardial infarction (STEMI) patients are associated with prognosis. This study investigated the feasibility of predicting left ventricular (LV) dysfunction in STEMI patients using an artificial intelligence (AI)-enabled ECG algorithm developed to diagnose STEMI. Serial ECGs from 637 STEMI patients were analyzed with the AI algorithm, which quantified the probability of STEMI at various time points. The time points included pre-PCI, immediately post-PCI, 6 h post-PCI, 24 h post-PCI, at discharge, and one-month post-PCI. The prevalence of LV dysfunction was significantly associated with the AI-derived probability index. A high probability index was an independent predictor of LV dysfunction, with higher cardiac death and heart failure hospitalization rates observed in patients with higher indices. The study demonstrates that the AI-enabled ECG index effectively quantifies ECG changes post-PCI and serves as a digital biomarker capable of predicting post-STEMI LV dysfunction, heart failure, and mortality. These findings suggest that AI-enabled ECG analysis can be a valuable tool in the early identification of high-risk patients, enabling timely and targeted interventions to improve clinical outcomes in STEMI patients.

Keyword ST-segment elevation myocardial infarction, Heart failure, Artificial intelligence, Electrocardiogram

Abbreviations

AMI	Acute myocardial infarction
AI	Artificial intelligence
AUROC	Area under the receiver operating characteristics curve
ECG	Electrocardiogram
IRB	Institutional Review Board
LV	Left ventricle
LVEF	Left ventricular ejection fraction
MVO	Microvascular obstruction
PCI	Percutaneous coronary intervention
STEMI	ST-segment elevation myocardial infarction

Acute myocardial infarction (AMI) is a leading cause of mortality worldwide¹. Prompt diagnosis and timely revascularization are crucial, especially ST-segment elevation myocardial infarction (STEMI)^{2,3}. Even with proper revascularization through percutaneous coronary intervention (PCI), some patients may experience

¹Department of Internal Medicine, Seoul National University College of Medicine and Department of Cardiology, Seoul National University Bundang Hospital, Seongnam, South Korea. ²Medical AI Co., Ltd, Seoul, South Korea. ³Artificial Intelligence and Big Data Research Center, Sejong Medical Research Institute, Bucheon, South Korea. ⁴These authors contributed equally: Ki-Hyun Jeon and Hak Seung Lee. ✉email: imcardio@gmail.com, cardiolee@gmail.com

left ventricular (LV) dysfunction, affecting both short- and long-term outcomes⁴. LV dysfunction is caused not only by myocardial injury during coronary occlusion, but also by reperfusion injury or microvascular obstruction (MVO) after revascularization^{5–7}. It is difficult to predict these events because they occur even if patency of the epicardial coronary artery is secured. Furthermore, no biomarkers are currently available to indicate the myocardial injury after revascularization.

Dynamic electrocardiogram (ECG) changes, such as the recovery of ST elevation after PCI, can reflect reperfusion at the myocardial level, not the vascular level, and have been linked with myocardial salvage and better outcomes^{8,9}. However, these various changes in ECG parameters are difficult to quantify and are currently interpreted by clinicians based on their observations.

Digital biomarkers are biometric data obtained through various digital health devices, and in a broader sense, data obtained by analyzing such data. Recent advancements in artificial intelligence (AI)-enabled ECG have shown remarkable efficacy in diagnosing and predicting cardiovascular disease^{10,11} by generating probability indices that serve as novel digital biomarkers for decision-making^{12,13}. This study aimed to evaluate the prognostic significance of the AI-based probability index derived from serial ECGs in patients who underwent primary PCI for STEMI.

Results

Serial ECG analysis in patients with STEMI following primary PCI

A total of 637 STEMI patients (mean age 64.7 ± 13.0 years, male 80.1%) were finally included in the analysis (Supplementary Fig. S1, online). The median probability index estimated by the AI-enabled ECG at various time points decreased over time after PCI and revealed significant differences ($P < 0.001$), with a value of 0.020 (interquartile range [IQR]: 0.018–0.032) at baseline, 0.975 (0.872–0.983) at Pre-PCI, 0.681 (0.043–0.969) at Immediate Post-PCI, 0.429 (0.034–0.945) at 6 h Post-PCI, 0.427 (0.036–0.954) at 24 h Post-PCI, 0.117 (0.026–0.876) at discharge, and 0.059 (0.024–0.503) at 1 M Post-PCI. Figures 1 shows the distribution of the probability index in predicting STEMI. Before primary PCI, most patients had values close to 1, whereas after PCI, this distribution is left-shifted towards 0.

Association between the probability index and LV dysfunction

In terms of predicting LV dysfunction, the AUROC was found to be the highest for the 6 h Post-PCI time point (Supplementary Fig. S2, Table S1, online). Consequently, this specific index was chosen as the basis for further analysis. To assess the relationship between the 6 h Post-PCI index and LV dysfunction, patients were stratified into tertiles based on the index; the cutoff points for the tertiles were 0.058 and 0.873. Table 1 shows the baseline characteristics according to the probability index. The mean LVEF after primary PCI of the low tertile group was $53.3 \pm 8.8\%$, $47.6 \pm 10.4\%$ for the middle tertile group, and $46.3 \pm 9.5\%$ for the high tertile group (ANOVA

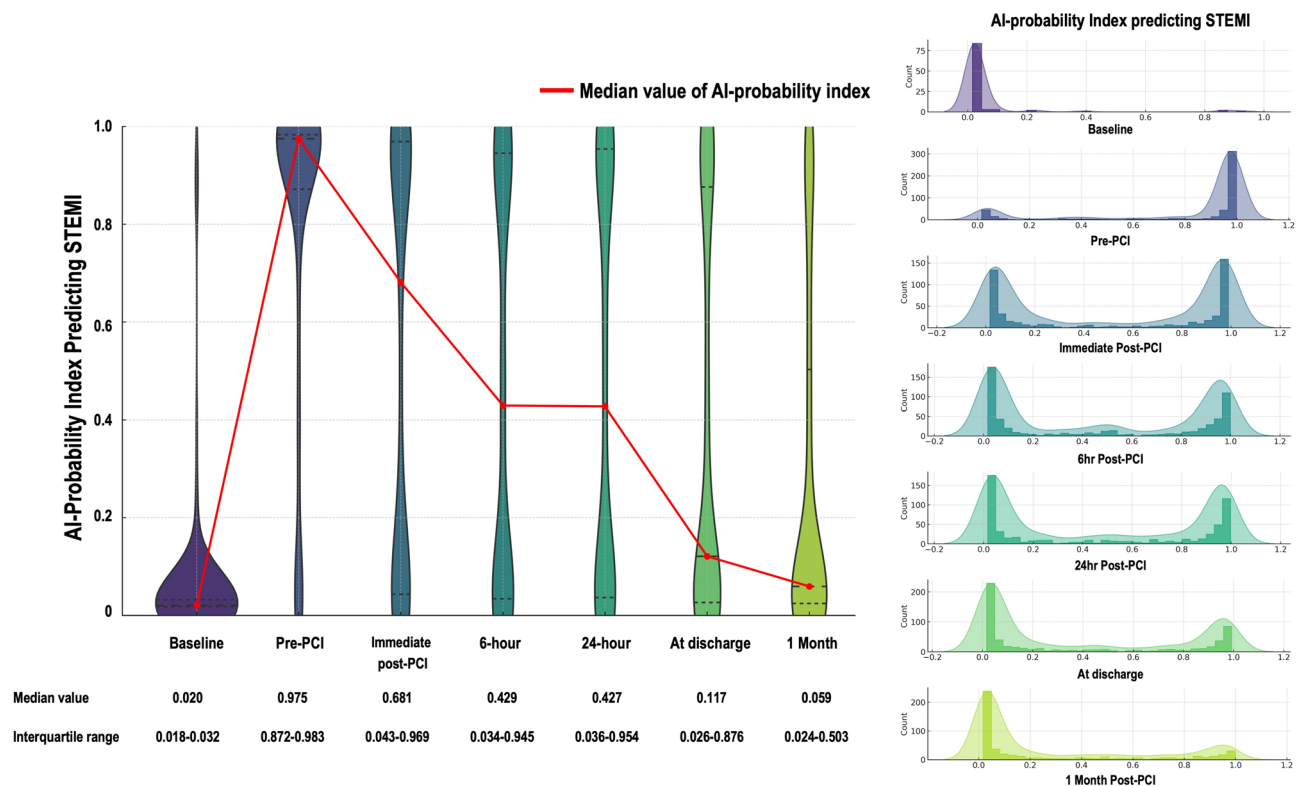


Figure 1. Distribution of the probability index predicting STEMI. STEMI, ST elevated myocardial infarction.

	AI-probability index			P value
	Low tertile (n=212)	Middle tertile (n=212)	High tertile (n=213)	
Age, years	64.9 ± 12.5	64.1 ± 12.6	65.2 ± 13.9	0.658
Female, n (%)	41 (19.8)	44 (20.8)	42 (19.7)	0.931
BMI, kg/cm ²	24.9 ± 3.5	24.2 ± 3.6	24.3 ± 3.1	0.139
Hypertension, n (%)	117 (55.2)	120 (56.6)	114 (53.5)	0.815
Diabetes, n (%)	66 (31.1)	57 (26.9)	75 (35.2)	0.179
ESRD, n (%)	3 (1.4)	3 (1.4)	3 (1.4)	0.999
Prior PCI, n (%)	9 (4.2)	7 (3.3)	8 (3.8)	0.878
Prior CVA, n (%)	15 (7.1)	16 (7.5)	17 (8.0)	0.939
Systolic BP, mmHg	131.1 ± 38.1	132.3 ± 35.2	133.4 ± 32.0	0.803
Diastolic BP, mmHg	77.2 ± 25.1	78.8 ± 24.0	78.8 ± 22.0	0.716
Pulse rate, bpm	72.4 ± 22.8	77.4 ± 20.7	81.4 ± 21.9	<0.001
Killip Class, n (%)				0.041
I	173 (81.6)	174 (82.1)	156 (73.2)	
II	18 (8.5)	17 (8.0)	26 (12.2)	
III	11 (5.2)	10 (4.7)	13 (6.1)	
IV	10 (4.7)	11 (5.2)	18 (8.5)	
Disease severity, n (%)				0.680
1 VD	96 (45.3)	105 (49.5)	94 (44.1)	
2 VD	68 (32.1)	67 (31.6)	67 (31.5)	
3 VD	48 (22.6)	40 (18.9)	52 (24.4)	
Infarct-related artery, n (%)				<0.001
LM	10 (4.7)	6 (2.8)	1 (0.5)	
LAD	82 (38.7)	135 (63.7)	134 (62.9)	
LCx	32 (15.1)	16 (7.5)	9 (4.2)	
RCA	88 (41.5)	55 (25.9)	69 (32.4)	
Peak troponin I, ng/ml	51.5 ± 43.8	74.9 ± 46.5	86.2 ± 42.5	<0.001
NT-proBNP, pg/dl	1682.2 ± 5631.8	1908.7 ± 5369.1	2543.5 ± 5668.7	0.259
Hemoglobin, g/dl	14.1 ± 2.1	14.2 ± 2.0	14.1 ± 2.2	0.765
Platelet, 10 ³ /μl	236.4 ± 66.8	238.0 ± 70.1	241.9 ± 81.1	0.728
eGFR, ml/min/1.73m ²	69.6 ± 25.1	71.8 ± 24.3	69.0 ± 24.9	0.457
Cholesterol, mg/dl	151.9 ± 46.1	155.4 ± 39.8	163.0 ± 48.6	0.034
Triglyceride, mg/dl	166.0 ± 150.6	168.1 ± 144.5	158.2 ± 126.8	0.751
HDL, mg/dl	45.2 ± 11.2	45.0 ± 11.7	45.8 ± 10.8	0.783
LDL, mg/dl	108.9 ± 37.7	110.5 ± 37.3	120.0 ± 39.2	0.005
CRP, mg/dl	0.8 ± 2.5	0.9 ± 2.6	1.4 ± 3.0	0.066

Table 1. Baseline characteristics according to the AI-probability index. AI, artificial intelligence; BMI, body mass index; BP, blood pressure; CRP, C-reactive protein; CVA, cerebrovascular accident; eGFR, estimated glomerular filtration rate; ESRD, end-stage renal disease; HDL, high density lipoprotein; LAD, left anterior descending artery; LCx, left circumflex artery; LDL, low density lipoprotein; LM, left main; NT-proBNP, N-terminal pro b-type natriuretic peptide; PCI, percutaneous coronary intervention; RCA, right coronary artery; VD, vessel disease.

$P < 0.001$, Fig. 2A). The prevalence of LV dysfunction (LVEF < 50%) was 30.0%, 55.9%, and 65.4%, respectively ($P < 0.001$, Fig. 3, Supplementary Fig. S3, online). Follow-up echocardiography, conducted 3 to 6 months post-primary PCI, exhibited similar trends in LV dysfunction across the tertile groups ($58.3 \pm 8.6\%$, $52.4 \pm 10.9\%$, and $50.9 \pm 9.0\%$, respectively, ANOVA $P < 0.001$, Fig. 2B). In terms of LV remodeling, patients with increased LV chamber size were also most likely to be in the high tertile group (Supplementary Fig. S3, online).

The multivariate logistic regression analysis showed that a high probability index was an independent predictive factor for LV dysfunction after primary PCI and the odds ratio of the high tertile of the probability index was 2.285 (95% CI: 1.428–3.656, $P = 0.001$; Table 2). Furthermore, similar results were seen when LV dysfunction was defined as LVEF < 40% (Supplementary Table S2, online).

Clinical outcomes according to the probability index of STEMI

There was a total of 58 cases (9.1%) of cardiac death and heart failure hospitalization, with a higher frequency observed in the highest probability index group (7.5% in the low tertile group, 7.1% in the middle tertile group, and 12.7% in high tertile group, $P = 0.066$). According to the Kaplan–Meier survival curve, when divided into a low index group (low and middle tertile group) and a high index group (high tertile group), the rate of cardiac

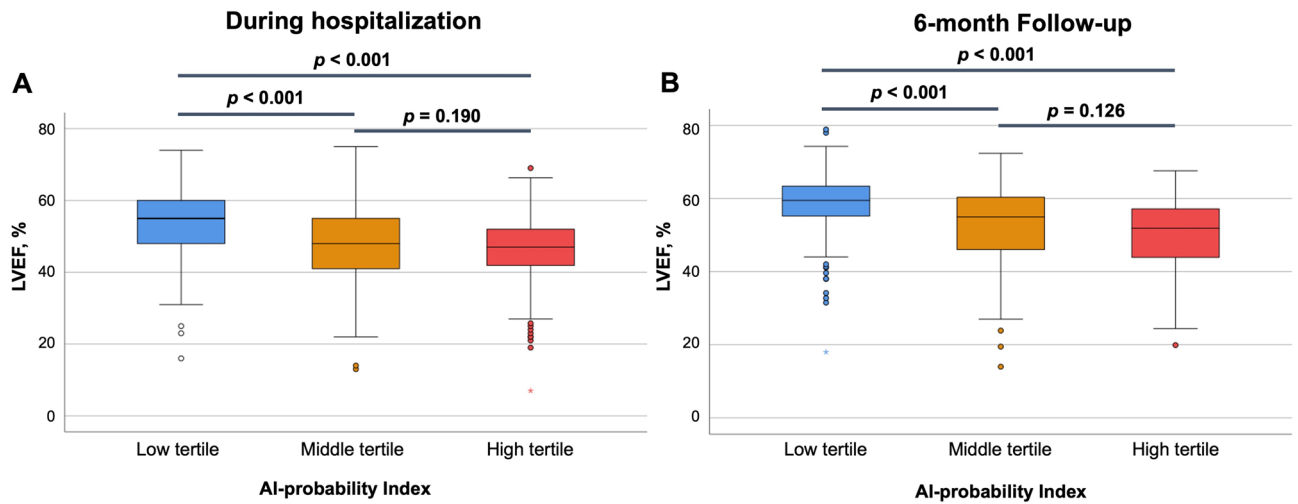


Figure 2. The mean LVEF after primary PCI according to the AI-probability index. AI, artificial intelligence; LVEF, left ventricular ejection fraction; PCI, percutaneous coronary intervention.

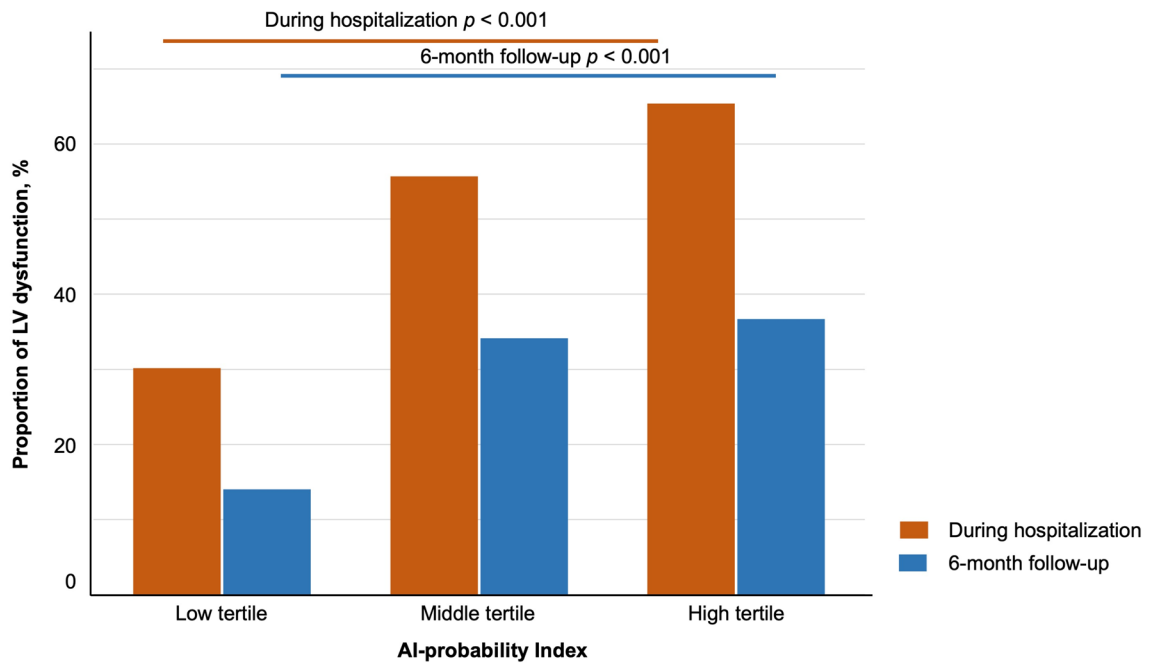


Figure 3. Proportion of LV dysfunction according to the AI-probability index. AI, artificial intelligence; LV, left ventricular.

death and heart failure hospitalization were significantly higher in the high index group (Log-rank $P = 0.024$, unadjusted HR = 1.766, 95% CI: 1.054–2.958; Fig. 4).

Discussion

The main finding of our study is that it is possible to quantify dynamic ECG changes in patients with STEMI after primary PCI using an AI-enabled ECG for STEMI detection. Furthermore, we could predict LV dysfunction and mortality in these patients by using these indices as a digital biomarker. To our knowledge, this is the first study to utilize a diagnostic AI-enabled ECG algorithm as a biomarker to predict prognosis.

During the thrombolysis era, it is impossible to confirm the patency of the coronary artery visually; thus, changes in the ECG were considered to be vital indicators of reperfusion, and several studies have focused on their prognostic implications^{8,14}. The dynamics of ECG changes have often provided insights into the adequate reperfusion to the myocardial level following thrombolytic therapy¹⁵. In addition, Dizon et al. showed that the ST segment resolution after primary PCI was significantly correlated with infarct size and MVO¹⁶.

While primary PCI effectively ensures patency of the epicardial artery, it does not necessarily guarantee complete perfusion at the myocardial level. The procedure can be associated with reperfusion injury, characterized

	Univariate analysis			Multivariate analysis		
	Odds ratio	95% CI	P value	Odds ratio	95% CI	P value
AI-probability index low tertile	Reference			Reference		
AI-probability index middle tertile	1.367	0.981–1.905	0.064	1.869	1.166–2.998	0.009
AI-probability index high tertile	2.549	1.807–3.594	<0.001	2.009	1.228–3.287	0.005
Age, years	1.006	0.994–1.018	0.344			
Body mass index, kg/cm ²	0.904	0.861–0.949	<0.001	0.902	0.849–0.959	0.001
Female	1.301	0.768–2.206	0.203			
Systolic blood pressure, mmHg	0.992	0.987–0.997	<0.001	0.986	0.975–0.997	0.015
Diastolic blood pressure, mmHg	0.992	0.986–0.999	0.023			
Pulse rate, bpm	1.019	1.011–1.026	<0.001	1.019	1.009–1.030	<0.001
Killip ≥ Class 3	2.852	1.659–4.902	<0.001	2.674	1.356–5.273	0.005
Hypertension	0.855	0.625–1.169	0.326			
Diabetes	1.128	0.805–1.580	0.484			
End-stage renal disease	1.981	0.491–7.991	0.337			
PCI to LM and/or LAD	2.564	1.854–3.546	<0.001	2.903	1.926–4.377	<0.001
eGFR, ml/min/1.73m ²	0.989	0.983–0.996	0.001			
Peak troponin I	1.016	1.012–1.020	<0.001	1.018	1.013–1.022	<0.001
C-reactive protein, mg/dl	1.250	1.107–1.412	<0.001	1.211	1.056–1.389	0.006
Cholesterol, mg/dl	1.003	0.999–1.006	0.131	1.006	1.000–1.012	0.043
LDL cholesterol, mg/dl	1.001	0.997–1.006	0.485			

Table 2. Independent risk factors for post-STEMI LV dysfunction. AI, artificial intelligence; CI, confidence interval; PCI, percutaneous coronary intervention; LAD, left anterior descending artery; LDL, Low density lipoprotein; LM, left main coronary artery.

by oxidative stress and inflammatory responses, leading to further myocardial damage¹⁷. On a cellular level, prolonged ischemia–reperfusion injury may lead to cell death, including apoptosis, autophagy, necrosis, and necroptosis^{18,19}. Microvascular obstruction (MVO) can also occur after PCI, preventing adequate myocardial level perfusion despite the opening of epicardial arteries. MVO can result from mechanical obstruction by a thrombus, embolus, or edema, and is associated with an adverse prognostic impact^{20,21}. Restoring blood flow at the macrovascular level through successful PCI achieving a thrombolysis in myocardial infarction flow score of 3 may not always translate to effective reperfusion at the myocardial level due to reperfusion injury and MVO²². They can compromise myocardial salvage despite the restoration of epicardial blood flow. ECG changes can confirm reperfusion at the myocardial level, but ECG changes are challenging to quantify, so they cannot be widely utilized as a prognostic factor.

The recent advancements in the AI-enhanced ECG algorithm allows the prediction of several diseases or medical conditions, such as LV dysfunction, valvular heart disease, anemia, and electrolyte abnormalities or renal impairment^{23–26}. The AI algorithm can extract subtle patterns and changes from ECG signals and provide quantified probability values between 0 and 1 for target diseases or conditions. These probability values can be utilized as digital biomarkers, allowing for a more precise and timely diagnosis, prognosis, and risk stratification. The AI algorithm used in this study is a deep-learning algorithm that diagnoses STEMI using a 12-lead ECG. The accuracy of the diagnosis was confirmed to be 95.7% in the external validation^{10,27}. We obtained a STEMI probability index from the serial ECGs over time after primary PCI using this algorithm. The algorithm can provide information about the ischemic burden at the myocardial level in STEMI patients after primary PCI, and this study was conducted to extend the prognostic predictive ability of this algorithm. We used it as a digital biomarker, which showed to be a good predictor of LV dysfunction and mortality after STEMI. The ECG at 6 h after primary PCI showed the highest predictive power. This result can be reasonable when considering the fact that revascularization should be performed within 12 h of symptom onset to salvage the myocardium.

Although it is possible to develop another algorithm to predicts LV dysfunction, in this study we applied the STEMI probability index to post-PCI ECGs to find that AI-enabled ECG algorithms can serve not only for binary decisions but also as biomarkers for diagnosis and predicting prognosis.

Several limitations of the present study are noteworthy. First, due to the retrospective nature of the study design, the timing of the ECG checks was not strictly standardized. We collected ECG data based on a window of approximately ± 3 h for our analysis. Second, our sample size was relatively small to substantiate differences in clinical outcomes in patients with STEMI. To generalize the results of this study, we believe that validation should be performed on a larger number of patients from different countries and ethnicities.

For this reason, we conducted our analysis with LV dysfunction as the primary endpoint. Third, as this is a study of reperfusion at the myocardial level in patients with STEMI, it would have been better to check infarct size measurements or MVO by cardiac magnetic resonance imaging; however, there are no data on this. Based on the findings of this study, we plan to conduct subsequent prospective research to validate the impact on clinical outcomes and correlation with cardiac image data.

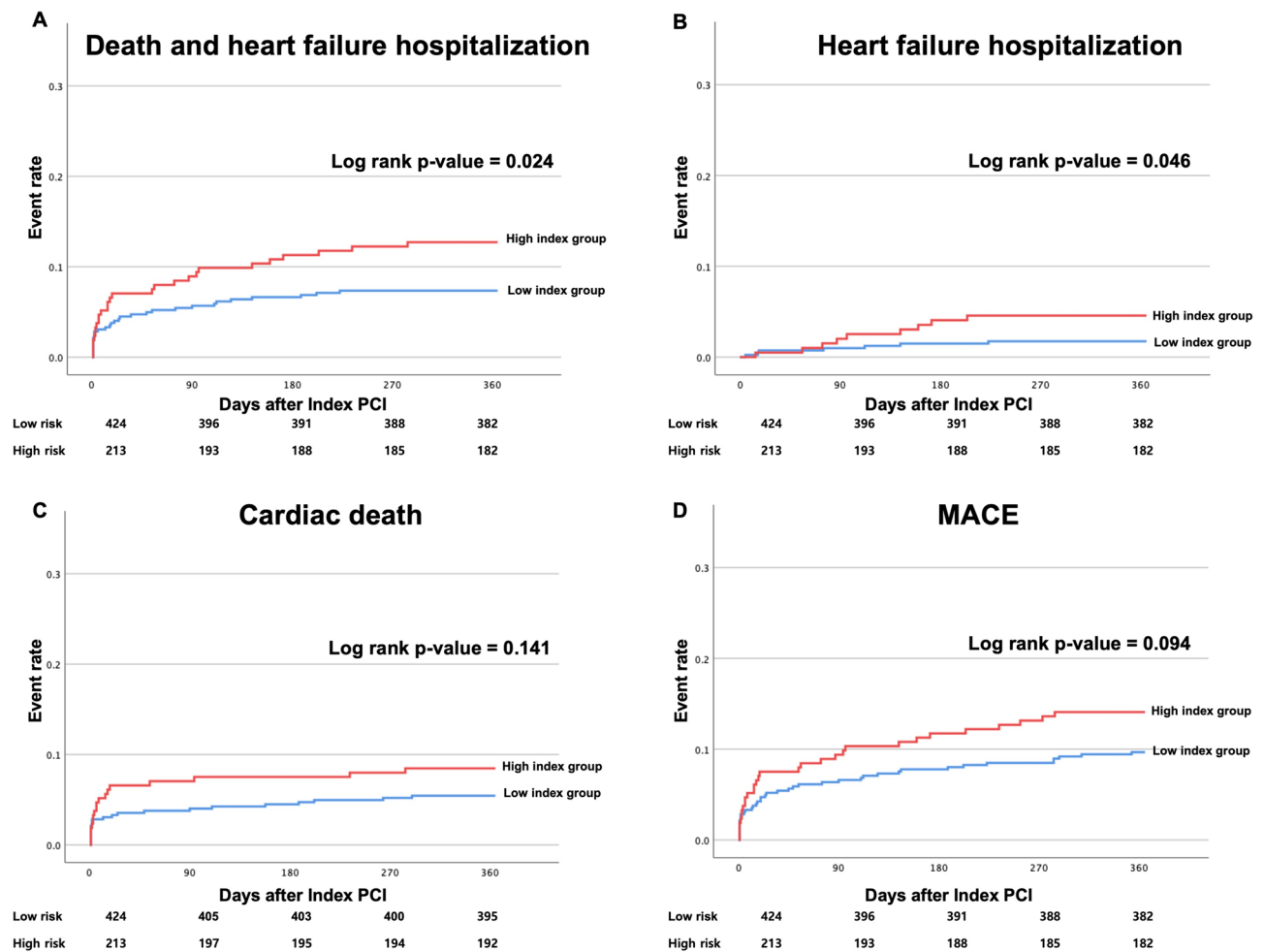


Figure 4. Clinical outcomes according to the AI-probability index. AI, artificial intelligence.

In conclusion, this study shows that the ECG digital biomarker from an AI-enabled ECG algorithm is an effective tool for quantifying ECG changes after primary PCI in patients with STEMI. The digital biomarker can predict post-AMI heart failure and is associated with clinical outcomes, indicating its potential as a prognostic marker. Further studies are needed to validate our results and explore the use of the digital biomarker in assessing myocardial reperfusion after primary PCI.

Methods

Study design and population

This retrospective study was designed to validate the prognostic value of an AI-enabled ECG derived probability index as a digital biomarker for predicting the prognosis of patients with STEMI after primary PCI. We retrospectively included consecutive patients who underwent primary PCI for STEMI between January 2019 and June 2022 in our institution. STEMI was diagnosed by a new ST segment elevation in ≥ 2 contiguous leads, measuring >0.2 mV in leads V1-3 or 0.1 mV in all other leads on a 12-lead ECG in a patient with the acute onset of chest pain or dyspnea. Patients who died within 24 h, those who underwent coronary artery bypass grafting, and patients for whom adequate serial ECGs could not be obtained were excluded from the study. This study was approved by the Institutional Review Board (IRB) of Biomedical Research Institute in Seoul National University.

Bundang Hospital (B-2201-733-104) and all methods were performed in accordance with the relevant guideline and regulation. The requirement for informed consent was waived by the IRB because of the retrospective study design using fully anonymized ECG and health data, with minimal potential harm.

Development of an AI-enhanced ECG prediction model for STEMI

In previous research, we developed a deep-learning algorithm for the detection of AMI and STEMI using a 12-lead ECG^{10,27}. The performance of this algorithm was validated, substantiating its efficacy. The output values, situated between 0 and 1, denote that an elevated value corresponds to an increased probability of the presence of AMI or STEMI. Data were sourced from two different hospitals for internal and external validation. A total of 22,259 ECGs (13,916 ECGs of non-AMI and 8,343 ECGs of AMI) from 15,113 patients were used to develop and validate the model. The area under the receiver operating characteristics curve (AUROC) was 0.927 (95% confidence interval [CI]: 0.908–0.945) for AMI and 0.983 (95% CI: 0.976–0.989) for STEMI.

We developed a ResNet-based model using PyTorch and Python, which is typically applied in image recognition, to classify ECG data by recognizing complex patterns. ECG classification is challenging because it involves deciphering rhythm and morphological features, both in image and time series analysis. Figure 5 shows the architecture of our deep-learning model, which includes a stem block, followed by six residual blocks, and ends with a fully connected layer to discern these patterns. Features from the ECG are progressively extracted through each block. We grouped every two residual blocks into what we call a "stage"; our model comprises three such stages. Within each residual block, we arranged a sequence of layer: a one dimensional (1D) convolutional layer, batch normalization, ReLU activation, another 1D convolutional layer, additional batch normalization, a dropout layer, and a skip connection. The stem block has a single layer plus a skip connection and max pooling. For training, we chose the Adam optimizer paired with a cosine warm-up optimization scheduler to adjust the weights and focal loss function for learning. We ran this scheduler for 150 epochs to test different hyperparameters and determine the best model structure, focusing on the highest area under the receiver operating characteristics (AUROC).

Data collection and analysis of serial ECGs

Serial ECGs were analyzed at multiple time points to quantify the dynamic ECG change and to evaluate myocardial reperfusion following primary PCI in patients with STEMI. The AI-enabled ECG quantified the probability of STEMI at each time points as a continuous variable between 0 and 1, i.e., as a digital biomarker. The time points at which the ECG was taken were as follows (Supplementary Fig. S4):

More than 1 month prior to the STEMI event (Baseline)
 Time of arrival to the emergency department prior to PCI (Pre-PCI)
 Immediately after primary PCI (Immediate Post-PCI)
 Six hours after PCI (6 h Post-PCI)
 Twenty-four hours after PCI (24 h Post-PCI)
 Time of discharge (At discharge)
 One month following the PCI (1 M Post-PCI)

Echocardiographic assessments were usually performed the day after primary PCI and follow-up echocardiography was performed around 6 months after the onset of STEMI. LV end systolic volume, LV end diastolic volume, and LV ejection fraction (LVEF) were estimated using the bi-planar modified Simpson's rule from apical two and four chamber views.

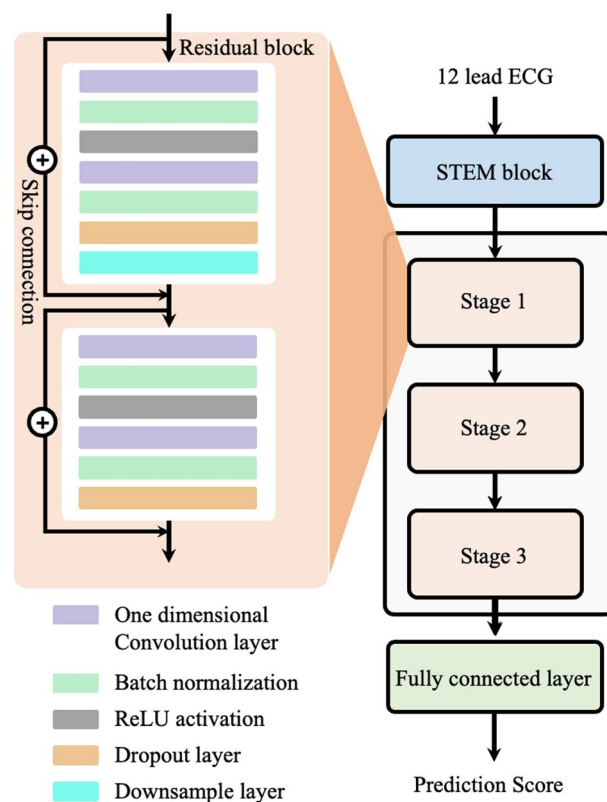


Figure 5. Architecture of the deep learning model. We utilized a ResNet-based model to predict AMI and STEMI. It consists of three parts: a stem block, stage block, and a full connected layer. AMI, acute myocardial infarction; STEMI, ST elevated myocardial infarction.

Study endpoint

The primary endpoint was post-STEMI LV dysfunction, defined as a LVEF < 50% during hospitalization and at the 6-month follow-up. The secondary endpoint was cardiac death or heart failure hospitalization within 1 year of the primary PCI. Cardiac death was defined as a mortality with a defined cardiovascular cause and heart failure hospitalization was defined as admission for ≥ 24 h with a primary diagnosis of heart failure, with ≥ 1 symptom and ≥ 2 physical examination, laboratory, or invasive findings of heart failure, and receives a heart failure-specific treatment²⁸.

Statistical analysis

Continuous variables are presented as mean (\pm standard deviation) and were compared using the unpaired and paired Student's t-test or Mann–Whitney *U* test. Means of tertile groups were compared by analysis of variance (ANOVA). Categorical variables are expressed as frequencies and percentages and were compared using the Pearson χ^2 test or Fisher's exact test when the Cochran rule was not met. For the analysis of probability index values obtained at different time points, we used the median value and the statistical significance of differences in these median values across various time points was evaluated using the non-parametric Kruskal–Wallis H-test. Univariate and multivariate logistic regression analyses were performed to identify the proportional hazard risk for LV dysfunction in patients with STEMI after primary PCI, which were adjusted for known potential confounders (age, sex, body mass index, systolic blood pressure, diastolic blood pressure, pulse rate, Killip class ≥ 3 , hypertension, diabetes mellitus, end stage renal disease, multiple vessel coronary artery disease, and infarct-related artery). Statistical significance was set at *P*-value < 0.05. All statistical analyses were performed using IBM/SPSSv24.0 (IBM/SPSS, Chicago, IL, USA), RStudio (Integrated Development Environment for R. RStudio, PBC, Boston, MA, USA), and Python (Python Software Foundation, Wilmington, DE, USA).

Data availability

The datasets used and/or analyzed in this study are available from the corresponding author upon reasonable request and to the extent permitted by the Personal Information Protection Act of Korea.

Received: 21 February 2024; Accepted: 12 July 2024

Published online: 17 July 2024

References

- Salari, N. *et al.* The global prevalence of myocardial infarction: a systematic review and meta-analysis. *BMC Cardiovasc. Disord.* **23**, 206. <https://doi.org/10.1186/s12872-023-03231-w> (2023).
- Lee, S. H., Hong, Y. J., Ahn, Y. & Jeong, M. H. Past, present, and future of management of acute myocardial infarction. *J. Cardiovasc. Interv.* **2**, 51–65 (2023).
- De Luca, G., Suryapranata, H., Ottervanger, J. P. & Antman, E. M. Time delay to treatment and mortality in primary angioplasty for acute myocardial infarction: Every minute of delay counts. *Circulation* **109**, 1223–1225. <https://doi.org/10.1161/01.CIR.0000121424.76486.20> (2004).
- Frantz, S., Hundertmark, M. J., Schulz-Menger, J., Bengel, F. M. & Bauersachs, J. Left ventricular remodelling post-myocardial infarction: Pathophysiology, imaging, and novel therapies. *Eur. Heart J.* **43**, 2549–2561. <https://doi.org/10.1093/eurheartj/ehac223> (2022).
- Ibanez, B., Heusch, G., Ovize, M. & Van de Werf, F. Evolving therapies for myocardial ischemia/reperfusion injury. *J. Am. Coll. Cardiol.* **65**, 1454–1471. <https://doi.org/10.1016/j.jacc.2015.02.032> (2015).
- Schroder, R. Prognostic impact of early ST-segment resolution in acute ST-elevation myocardial infarction. *Circulation* **110**, e506–510. <https://doi.org/10.1161/01.CIR.0000147778.05979.E6> (2004).
- Heusch, G. Coronary microvascular obstruction: the new frontier in cardioprotection. *Basic Res. Cardiol.* **114**, 45. <https://doi.org/10.1007/s00395-019-0756-8> (2019).
- de Lemos, J. A. & Braunwald, E. ST segment resolution as a tool for assessing the efficacy of reperfusion therapy. *J. Am. Coll. Cardiol.* **38**, 1283–1294. [https://doi.org/10.1016/s0735-1097\(01\)01550-9](https://doi.org/10.1016/s0735-1097(01)01550-9) (2001).
- Dong, Q. *et al.* ST-segment resolution as a marker for severe myocardial fibrosis in ST-segment elevation myocardial infarction. *BMC Cardiovasc. Disord.* **21**, 455. <https://doi.org/10.1186/s12872-021-02269-y> (2021).
- Lee, B. T. *et al.* Usefulness of deep-learning algorithm for detecting acute myocardial infarction using electrocardiogram alone in patients with chest pain at emergency department: DAMI-ECG study. *J. Cardiovasc. Interv.* **2**, 100–112 (2023).
- Attia, Z. I., Harmon, D. M., Behr, E. R. & Friedman, P. A. Application of artificial intelligence to the electrocardiogram. *Eur. Heart J.* **42**, 4717–4730. <https://doi.org/10.1093/eurheartj/ehab649> (2021).
- Ito, S. *et al.* Correlation between artificial intelligence-enabled electrocardiogram and echocardiographic features in aortic stenosis. *Eur. Heart J. Digit. Health* **4**, 196–206. <https://doi.org/10.1093/ehjdh/ztad009> (2023).
- Jeon, K.-H. *et al.* Identifying atrial fibrillation with sinus rhythm electrocardiogram in embolic stroke of undetermined source: A validation study with insertable cardiac monitors. *Korean Circ. J.* **53**, 758–771 (2023).
- von Essen, R. *et al.* Myocardial infarction and thrombolysis Electrocardiographic short term and long term results using precordial mapping. *Br. Heart J.* **54**, 6–10. <https://doi.org/10.1136/hrt.54.1.6> (1985).
- Vaturi, M. & Birnbaum, Y. The use of the electrocardiogram to identify epicardial coronary and tissue reperfusion in acute myocardial infarction. *J. Thromb. Thrombol.* **10**, 137–147. <https://doi.org/10.1023/a:1018762509887> (2000).
- Dizon, J. M. *et al.* Relationship between ST-segment resolution and anterior infarct size after primary percutaneous coronary intervention: Analysis from the INFUSE-AMI trial. *Eur. Heart J. Acute Cardiovasc. Care* **3**, 78–83. <https://doi.org/10.1177/2048872613508658> (2014).
- Frohlich, G. M., Meier, P., White, S. K., Yellon, D. M. & Hausenloy, D. J. Myocardial reperfusion injury: Looking beyond primary PCI. *Eur. Heart J.* **34**, 1714–1722. <https://doi.org/10.1093/eurheartj/ehu090> (2013).
- Wu, M. Y. *et al.* Current mechanistic concepts in ischemia and reperfusion injury. *Cell Physiol. Biochem.* **46**, 1650–1667. <https://doi.org/10.1159/000489241> (2018).
- Heusch, G. Myocardial ischaemia-reperfusion injury and cardioprotection in perspective. *Nat. Rev. Cardiol.* **17**, 773–789. <https://doi.org/10.1038/s41569-020-0403-y> (2020).
- Bonfig, N. L. *et al.* Increasing myocardial edema is associated with greater microvascular obstruction in ST-segment elevation myocardial infarction. *Am. J. Physiol. Heart Circ. Physiol.* **323**, H818–H824. <https://doi.org/10.1152/ajpheart.00347.2022> (2022).

21. Abbas, A. *et al.* Cardiac MR assessment of microvascular obstruction. *Br. J. Radiol.* **88**, 20140470. <https://doi.org/10.1259/bjr.20140470> (2015).
22. Gassler, J. P. & Topol, E. J. Reperfusion revisited: beyond TIMI 3 flow. *Clin. Cardiol.* **22**, 20–29. <https://doi.org/10.1002/clc.4960221605> (1999).
23. Kwon, J. M. *et al.* Development and validation of deep-learning algorithm for electrocardiography-based heart failure identification. *Korean Circ. J.* **49**, 629–639. <https://doi.org/10.4070/kcj.2018.0446> (2019).
24. Kwon, J. M. *et al.* Deep learning-based algorithm for detecting aortic stenosis using electrocardiography. *J. Am. Heart Assoc.* **9**, e014717. <https://doi.org/10.1161/JAHA.119.014717> (2020).
25. Kwon, J. M. *et al.* A deep learning algorithm to detect anaemia with ECGs: A retrospective, multicentre study. *Lancet Digit. Health* **2**, e358–e367. [https://doi.org/10.1016/S2589-7500\(20\)30108-4](https://doi.org/10.1016/S2589-7500(20)30108-4) (2020).
26. Kwon, J. M. *et al.* Artificial intelligence assessment for early detection and prediction of renal impairment using electrocardiography. *Int. Urol. Nephrol.* **54**, 2733–2744. <https://doi.org/10.1007/s11255-022-03165-w> (2022).
27. Cho, Y. *et al.* Artificial intelligence algorithm for detecting myocardial infarction using six-lead electrocardiography. *Sci. Rep.* **10**, 20495. <https://doi.org/10.1038/s41598-020-77599-6> (2020).
28. Abraham, W. T. *et al.* Standardized definitions for evaluation of heart failure therapies: Scientific expert panel from the heart failure collaborative and academic research consortium. *JACC Heart Fail* **8**, 961–972. <https://doi.org/10.1016/j.jchf.2020.10.002> (2020).

Author contributions

HSL contributed to the conceptualization, methodology and wrote the first draft. SK and JHJ were involved methodology, data analysis and AI model development. YYJ, JMS, and MSL contributed to AI model development. JSK, HWC, SHK, WL, CHY, and JWS contributed methodology and clinical data collection and verified the clinical coding. TJY and IHC contributed conceptualization and supervised the project. KHJ and JMK were the principal investigators, contributed to the study idea and design, prepared and verified the clinical coding, performed data analysis, wrote the first draft, and contributed to the subsequent drafts.

Competing interests

Medical AI Inc. provided support in the form of salaries for authors (Hak Seung Lee, Sora Kang, Jong-Hwan Jang, Yong-Yeon Jo, Jeong Min Son, Min Sung Lee, Joon-myung Kwon). Joon-myung Kwon is the founder and stakeholder in Medical AI Inc., a medical artificial intelligence company. Dr. Jeon have received research grant support from Medical AI Inc. Other authors have nothing to declare. There are no patents, products in development of marketed products to declare.

Additional information

Supplementary Information The online version contains supplementary material available at <https://doi.org/10.1038/s41598-024-67532-6>.

Correspondence and requests for materials should be addressed to K.-H.J. or H.S.L.

Reprints and permissions information is available at www.nature.com/reprints.

Publisher's note Springer Nature remains neutral with regard to jurisdictional claims in published maps and institutional affiliations.



Open Access This article is licensed under a Creative Commons Attribution 4.0 International License, which permits use, sharing, adaptation, distribution and reproduction in any medium or format, as long as you give appropriate credit to the original author(s) and the source, provide a link to the Creative Commons licence, and indicate if changes were made. The images or other third party material in this article are included in the article's Creative Commons licence, unless indicated otherwise in a credit line to the material. If material is not included in the article's Creative Commons licence and your intended use is not permitted by statutory regulation or exceeds the permitted use, you will need to obtain permission directly from the copyright holder. To view a copy of this licence, visit <http://creativecommons.org/licenses/by/4.0/>.

© The Author(s) 2024